Measuring Atmospheric Visibility by Digital Image Processing

Chin-Hsiang Luo[1]*, San-Ho Liu[2], Chung-Shin Yuan[2]

[1] *Department of Environmental Engineering, Hung-Kuang Institute of Technology*
No.34, Chung-Chie Rd., Sha-Lu, Taichung 433, Taiwan, R.O.C.
[2] *Institute of Environmental Engineering, National Sun Yat-Sen University*
No. 70, Lien-Hai Rd., Kaohsiung, Taiwan, R. O. C.

This study presents an approach to measure the atmospheric visibility of two areas in Taiwan - one located near Taichung and the other at Kaoshiung - by digital image processing. The approach includes the following four steps. First, take digital images of selected targets around these areas. Second, analyze the difference between the brightness (the gray level of the images) of the targets and that of atmospheric background using a computing program. Third, calculate the specific brightness defined as digital visibility. Finally, determine the relationship between specific brightness and atmospheric visibility.

The existence of a limit to human vision can be determined by investigating the visibility of two targets, the Da-du Mountain and the Western Shore, at different distances from Taichung Harbor Weather Station. Furthermore, a telephotographic investigation determines the specific brightness of the skyscraper at Kaoshiung. Its specific brightness (B_g) is closely related to the real-time visibility of the atmosphere (V_a) when visual range is from 5 to 10 km: $|B_g| = -0.2186\ V_a + 2.7035$, $r = 0.9079$. Our results show that this new index, specific brightness, can provide visibility measurement by accurate digital data. Furthermore, images of areas of interest can be established for future analysis, without the potential for discrepancy caused by humans.

Key Words: atmospheric visibility, digital image processing, specific brightness, gray level

1. Introduction

The clarity of view, called visibility, can influence the quality of life, human mood and the metropolitan tourism. The scientific definition of visibility is the maximum distance at which the outlines of selected targets can be recognized against the horizon as background (1). Reduced visibility strongly implies the atmospheric pollution. Ambient pollutants, particulate matter and gaseous species, can seriously decrease the visual range (2~6). Atmospheric visibility is frequently investigated for meteorological, traffic-related, airport-related and similar purposes.

*Corresponding author:
Tel : 886-4-26318652-1500
Fax : 886-4-26334695
E-mail address:andyluo@sunrise.hku.edu.tw

Prevailing visibility (7, 8) is a common measure of visual limitation in ambient environment. Trained observers stand in a specific position (for example, a weather station) to detect periodically selected targets in various directions. These targets are ideally black. If a target is not available, its color must be sufficiently dark to be distinguished from the background. The visibility equals the distance from which the farthest target can be recognized. Therefore, the accuracy of the above measurement is restricted by the distances among

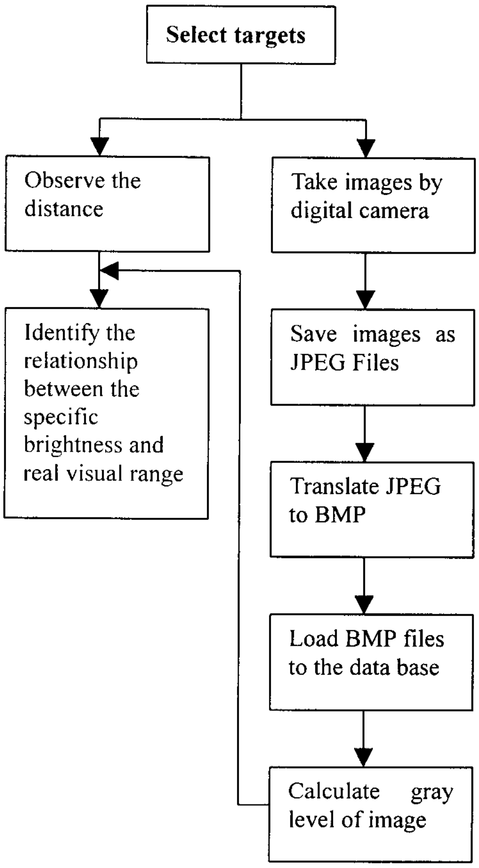

Figure 1: The diagram for our new methodology.

targets.

Some visibility models and modified formulas (9~12) have applied photographic processing to calculate or improve various parameters related to atmospheric visibility extensively. Accordingly, attempts have been made to determine the factors that affect visual range, including scattering properties, atmospheric conditions, colors of targets, size distributions of aerosols, pollutant compositions and so on. However, a complicated procedure appears to inadequately describe perceptibility of the environment in real-time.

Obviously, atmospheric visibility has been not only a concern of the public, but also a useful index for investigating variations in the atmosphere. This study presents a novel method to measure visibility by digital telephotography. Real-time digital visibility can be established using computer processing. The numbers of selected targets

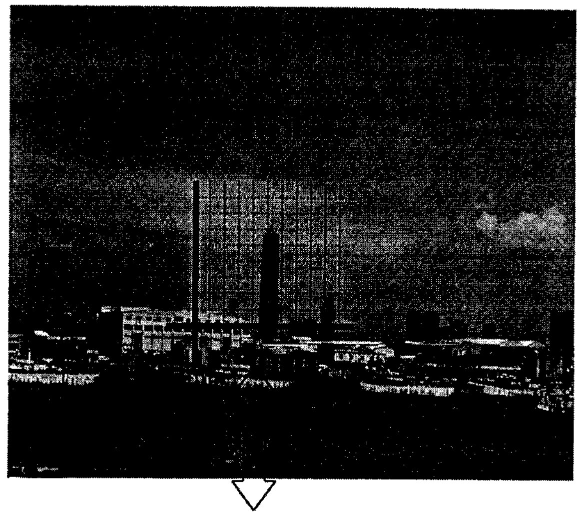

$$f(x,y)=\begin{bmatrix} f(0,B-1)\ldots\ldots\ldots\ldots f(A-1,B-1) \\ \ldots\ldots\ldots\ldots\ldots\ldots \\ \ldots\ldots\ldots\ldots\ldots\ldots \\ f(0,0)\ldots\ldots\ldots\ldots f(A-1,0) \end{bmatrix}$$

Figure 2: The mathematical translation between image and related matrix.

required to measure visibility, and the discrepancy caused by humans, are reduced.

2. Methodology

In this work, atmospheric visibility is measured by combining visual investigation by observers with digital telephotography. Figure 1 depicts the procedure.

Digital image processing includes several procedures (13). A monochrome digital image basically includes data concerning points in space and the relative brightness intensity (gray level). These data can be collected, mathematically translated to the following A×B matrix:

$$f(x,y)=\begin{bmatrix} f(0,B-1)\ldots\ldots\ldots\ldots f(A-1,B-1) \\ \ldots\ldots\ldots\ldots\ldots\ldots \\ \ldots\ldots\ldots\ldots\ldots\ldots \\ f(0,0)\ldots\ldots\ldots\ldots f(A-1,0) \end{bmatrix} \quad (1)$$

In this matrix, each elementary function represents the digital intensity of the selected point (also called pixel) on the image. Figure 2 shows the relationship between the image and the translated matrix.

An image consists of two orthogonal components, color and brightness. However, the difference between a target and the background, in ether color or brightness, determines whether the target is visible. Middleton (14) confirmed that the difference in brightness was more important, that is, difference between colors could be ignored at a large distance. Hence, analyzing only the brightness difference in the image is reasonable for measuring visibility.

Physiological research (13) employs Weber's ratio to clarify how a target or object is identified or distinguished from the surroundings (such as the atmospheric environment) by the human visual system. Weber's ratio, W_r, is defined as follows.

$$W_r = \frac{|I_t - I_b|}{I_b} \qquad (2)$$

where I_t and I_b are the light intensities of the target and background, respectively. The value of W_r expresses the critical condition at which the difference between the light intensity of the target and that of the background could result in 50% probability of perception of the target. The definition of W_r is extended to express the difference between the digital brightness between the target and the background, as the specific brightness, B_g:

$$B_g = \log\frac{|B_t - B_b|}{B_b} \qquad (3)$$

where, B_t and B_b are the digital brightnesses of the target and background, respectively. Horvath (1) presented a similar definition. The largest B_g discerned by humans is called the brightness threshold, up to which the distance between the target and the observer is called critical visibility, and is defined as the prevailing visibility. During normal daylight conditions, the threshold is independent of the brightness of the background (1). The range of the brightness threshold varies from -1.7 to -1.3. Unfortunately, most measurements cannot yield a unique brightness threshold (1).

This study developed a computer process which can transfer digital images of specific targets to values of B_g. The procedure includes the following steps. First, convert the colorful image into a special type of image file, BMP, which includes only the brightness of the image. Next, select the area of concern on the image to analyze the difference between the digital brightness (the gray level) of the target and the background, using Eq. 3. This process is also called segmentation. Finally, verify the relationship between the specific brightness and the real visual range.

3. Experimental

3.1 Locations

The survey was undertaken in two areas, one of which was Taichung Harbor Weather Station in the middle of Taiwan. The Da-du Mountain and the Western Shore were selected as the targets. The distance between Da-du Mountain (Western Shore) and the station is 10 (20) km. The sampling period was July 7-23, 1999.

The other area was located at a weather station of Kaohsiung, a city in southern Taiwan. A famous skyscraper in downtown was an excellent target, which had a distance of 5.3 km from the station. The four sampling periods were Jan. 28-Feb. 6, 1999; May 21-30, 1999; Jan. 8-16, 2000, and Mar. 24-30, 2000.

3.2 Equipment

The Kodak digital camera (DC 120) and Nikon digital camera (COOLPIX 900) were used to take images of targets. These automatic cameras, equipped with a triple-focus lens and a charge-

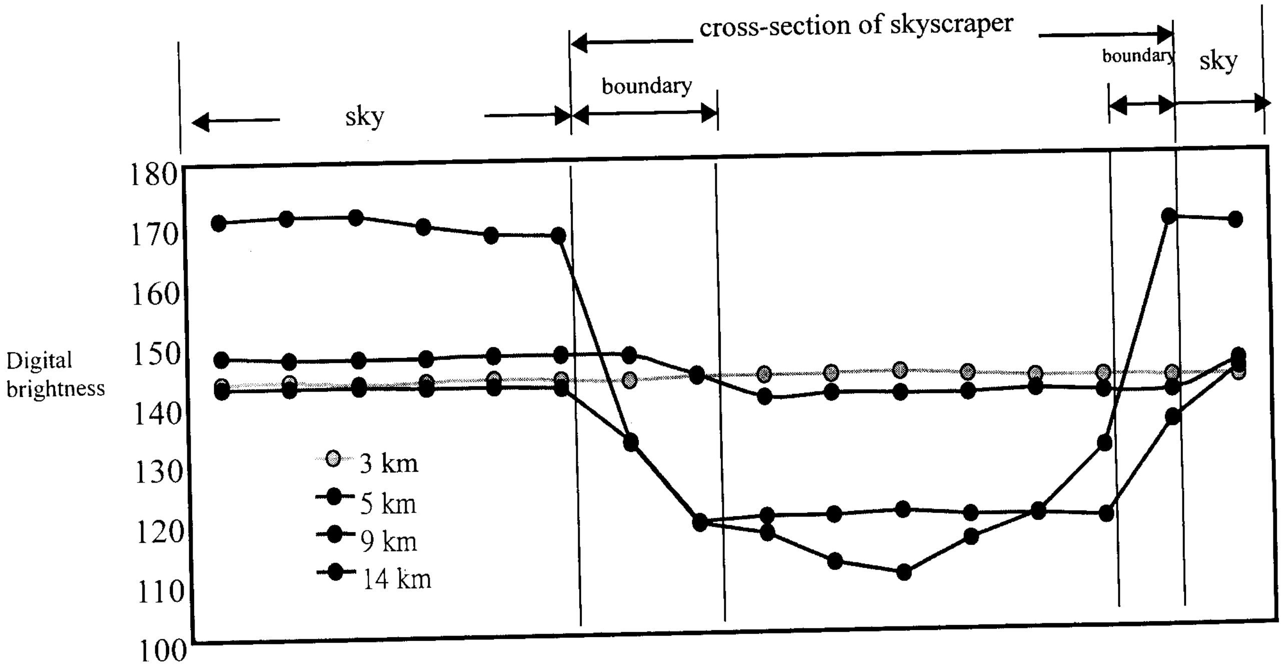

Figure 3: Variations of digital brightnesses of the cross-sectional image of the skyscraper and sky (background) at different visual range, 3-14 km

couple device (CCD), generated an image of 640×480 pixels. Trained observers simultaneously undertook a visual investigation. The distance between each selected target and the observers was appropriate to the visibility measurement. The distance between each selected target and the camera was also sufficiently large for the CCD detector. The camera and human eyes focused at infinity (∞). The lighting equipment of the camera was not used because images were obtained in the daytime.

3.3 Computer Processing

Each image was partitioned into 256×256 sub-regions, resulting in a total of 65536 pixels. Because each pixel needed an 8-bits of memory, and thus was associated with 2^8 digital numbers (DN). A pixel consists of three original colors, red, green and blue (RGB). The digital data deposited in every pixel on the image include the brightness of each of these original colors. The brightness of the color was defined as DN from 0 to 255. The brightness declined as DN increased. The transfer function converted the multicolored image to the related monochrome image by averaging the brightness of RGB (B_R, B_G, B_B) at each pixel. Mixing RGB could produce a colorless gray. The gray level value (GL) at each pixel was calculated as follows.

$$GL = \frac{B_R + B_G + B_B}{3} \qquad (4)$$

The GL was defined as the digital brightness and ranged from 0 to 255. Therefore, perfect black was represented by a GL= 0. In contract, GL= 255 represented pure white. The translating program modified the digital brightness (GL) of images. Then, the modified data were saved in the form of Eq. 1.

4. Results and Disscussion

4.1 Brightness Difference

Figure 3 presents the digital brightness of the skyscraper and the related background at the visual

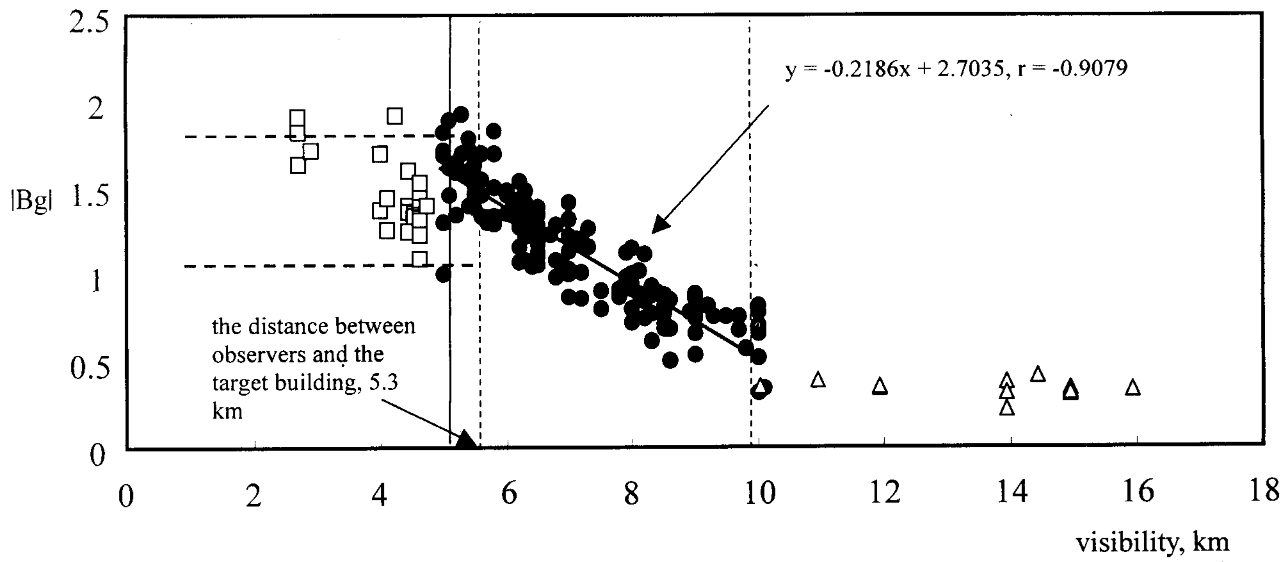

Figure 4: The relationship of the specific brightness with visibility for the skyscraper in Kaohsiung, Taiwan.

range of 3, 5, 9 and 14 km, respectively.

The digital brightness of the sky (background) was always constant for a given visual range and for most of the buildings. Two boundaries existed between the building and the sky. However, their brightness became vague as the visual range declined.

Obviously, the difference between the brightness of the building and that of sky was easily recognized when the visual range exceeded 5.3 km, the distance between the building and observers. When the visual range was smaller than 5.3 km, the difference in brightness could still be discerned, but the target became invisible to human eyes. Indeed, digital brightness data were more accurate than the data obtained from the naked eyes.

4.2 Specific Brightness

Empirical values of the specific brightness, B_g, for targets under various conditions of visibility were obtained from Eq. 3. Figure 4 illustrates that variation of the B_g values for the skyscraper depended on the visibility.

When the visibility was lower than 5.3 km, the skyscraper at Kaohsiung was invisible and the values of its B_g ranged from -1.0 to -1.5. In fact, when visibility was near 5 km, the mean B_g of the building approached -1.5. This finding is consistent with that in previous studies (1).

Table 1: Comparison between observation distance and brightness threshold for three targets.

Targets	Observation Distance	Brightness Threshold
Da-du Mountain	10 km	-1.06
Western Shore	20 km	-1.07
Skyscraper	5.3 km	-1.50

Measuring the B_g for the Da-du Mountain and the Western Shore near Taichung yielded similar results. The mean brightness threshold of the two targets near Taichung was about -1.1, although the distance to the Western Shore was double that to the Da-du Mountain. Consequently, visual limitation of the human eye was assumed to be constant.

Several potential factors, including discrepancies of observers, inhomogeneous distribution of aerosols, effluent from pollutant sources and so on, were supposed to influence the relationship between the observed distance and brightness threshold. Table 1 compares above relationships. At different locations, the values of brightness threshold differed from −1.06 to −1.50. Only minor deviations occurred. Under normal daylight conditions, previous results (1) showed that the brightness threshold was about -1.70, for a 50% probability of detection. With respect to airport visibility, the recommended brightness threshold is -1.30 (1).

When the visibility was between 5 and 10 km, B_g and visibility (V_a), as measured by observers for the skyscraper, were highly linearly correlated.

$$|B_g| = -0.2186V_a + 2.7035, \quad r = 0.9079 \tag{5}$$

Accordingly, only one target was needed to estimate the visibility at 10 km precisely.

At above 10 km visibility, this correlation disappeared. Fortunately, the clarity of the atmosphere is irrelevant under good conditions.

5. Conclusions

Visibility was measured, using digital image processing. Several new approaches were proved successfully. First, the difference between the digital brightness of selected targets and the background was eliminated as the visibility declined. Second, specific brightness was defined as digital visibility and the brightness threshold of the target was derived to represent the visual limitation of the human eye. The threshold appeared to be independent of the observation distances. Furthermore, the specific brightness and the visibility were highly linearly correlated within the visual range of 5 to 10 km. In summary, our research confirmed that measuring visibility using a camera-computer system was as effective as the real-time recording of weather investigators. With respect to measuring visibility in the metropolitan area, the results support the selection of targets and provide a real-time investigation of visibility and characteristic images of certain areas of interest without possible human error.

Acknowledgement

The authors would like to thank the National Science Council of the Republic of China for financially supporting this research under Contract No. NSC 88-2212-E-241-001. Dr. Uen, J. Y. would be appreciated for assistance in developing the computer processing program.

References

Horvath, H. Atmospheric Visibility. Atmospheric Environment **1981**, 15, 1785-1796.

Dzubay, T. E., Steven, R. K., Lewis, C. W., Hern, D. H., Courtney, W. J., Tesch, J. W. and Mason, M. A. Visibility and Aerosol Composition in Houston, Texas. Environmental Science and Technology **1982**, 16, 514-525.

Tsai, Y. I. and Cheng, M. T. Relationship between Visibility, Meteorological Factors, and Aerosol Composition in the Taichung Near-shore Area. 1997 International Conference on Aerosol Technology/Environmental Measurement and Control Proceedings **1997**, 76-84.

Yuan, C. S. and Yang, H. Y. A Study on the Relationship of Visibility with Suspended Particles and Meteorological Factors in Kaohsiung Metropolitan Area. 1997 International Conference on Aerosol Technology/Environmental Measurement and Control Proceedings **1997**, 334-354.

Pryor, S. C., Simpson, R. and Sakiyama, S. Visibility and Aerosol Composition in the Fraser Valley During Reveal. Journal of the Air & Waste Management Association **1997**, 47, 147-156

Sequeira, R. and Lai, K. H. The Effect of Meteorological Parameters and Aerosol Constituents on Visibility in Urban Hong Kong. Atmospheric Environment **1998**, 32, 2865-2877.

Hinds, W. C. *Aerosol Technology*. 2nd ed., John Wiley & Sons, Inc., 1999, 364-370.

Seinfeld, J. H. *Atmospheric Chemistry and Physics of Air Pollution*. John Wiley & Sons, Inc., 1986, 49-50.

Williams, M., Chan, L. Y. and Lewis, R. Validation and Sensitivity of a Simulated-Photograph Technique for Visibility Modelling. Atmospheric Environment **1981**, 15, 2151-2170.

Babson, B. L., Bergstrom, R. W., Samuelson, M. A., Seigneur, C., Waggoner, A., Malm, W. C. Statistical Analysis of Nephelometer Regional Field Data. Atmospheric Environment **1982**, 16, 2335-2346.

Malm, W. C., Molenar, J. V. Visibility Measurements in National Parks in the Western United States. Journal of the Air Pollution Control Association **1984**, 34, 899-904.

Larson, S. M., Cass, G. R., Hussey, K. J. and Luce, F. Verification of Image Processing Based Visibility Models. Environmental Science and Technology **1988**, 22, 629-637.

Gonzalez, R. C. and Woods, R. E. *Digital Image Processing*. Addison-Wesley Publishing Company, 1992.

Middleton, W. E. K. *Vision through the Atmosphere*, University of Toronto Press, Toronto, 1963.

Received for review, January 28,2002

Accepted, June 17, 2002

AAQR-2002-03